The Impacts of Mesoscale Dynamics on Cirrus Structure Evaluated Using a High-Resolution Mesoscale Model

M. M. Khaiyer and J. Verlinde
Pennsylvania State University
University Park, Pennsylvania

Introduction

A thorough understanding of the dynamics of cirrus cloud formation is needed in order to parameterize these clouds accurately in numerical models. The scales at which cirrus clouds develop affect their treatment within the coarse resolution climate models, which typically have grid-point separations on the order of 200 km. There is a considerable amount of evidence to show that small-scale development is a factor in cirrus formation. Observational studies have shown evidence of the development of cirrus convective elements on the mesoscale (e.g., Sassen et al. 1989). Gultepe and Starr (1995) documented from aircraft observations that waves of varying wavelengths, ranging from 2 km to over 100 km, were present in the sampled cirrus clouds. For this reason, gravity waves are the focus of this study.

Objectives for the Study

The case examined in this study is the November 26, 1991, Second ISCCP[(a)] Regional Experiment (FIRE-II) cirrus case, characterized by a jet streak propagating through the experiment region. The synoptic situation, as well as various features of the observed cloud system, has been described in detail in several papers (e.g., Mace et al. 1995; Westphal et al. 1996). The selection of this case allows for evaluation of the impacts of the mesoscale dynamics, which in this study will be related to the dynamics of the jet streak, on cirrus development. The development of gravity waves near the jet streak area is studied, with the following objectives for this work:

- to investigate the role of mesoscale dynamics on the formation of cirrus
- to evaluate possible causes of these mesoscale phenomena.

A better understanding of the above will allow for assessment of the ramifications of these mesoscale phenomena on cirrus parameterizations.

Model Description

The model used for this experiment is the non-hydrostatic version of the Pennsylvania State University/National Center for Atmospheric Research Mesoscale Model (PSU/NCAR MM5) (Dudhia 1993; Grell et al. 1994). A full atmospheric radiation package (Dudhia 1993) is incorporated, and the Reisner microphysical scheme (Reisner et al. 1997) is used with one modification: the Meyers scheme (Meyers et al. 1992) replaces the Fletcher's average approach for ice nucleation. The mixed-phase microphysical scheme implemented explicitly predicts ice, snow, cloud, and rain (Reisner et al. 1996). Ice sedimentation is also included (following Heymsfield and Donner 1990). A radiative boundary condition is imposed at the top of the model, allowing wave energy to pass through unreflected (Klemp and Durran 1983; Bougeault 1983).

Two grids are used within the model simulations (Figure 1). Forty-six half sigma levels (47 full sigma levels) of variable separations are used to achieve approximately 250-m vertical resolution within cirrus cloud levels (approximately 5 km above ground level [AGL] to 10.5 km AGL). Four-dimensional data assimilation (FDDA) (Stauffer and Seaman 1990) is employed to dynamically initialize the coarse mesh of the simulations via a 12-hr preforecast period).

Results

Simulation EXP, with a 36-km coarse-grid domain and a 12-km resolution inner domain, allows for the resolution of small-scale dynamical features. A control simulation (denoted CTRL), consisting of only the coarse-grid domain, is used to verify that the features produced with the higher resolution grid are not merely the result of the model-imposed boundary between Domains 1 and 2. Model simulations are integrated

(a) International Satellite Cloud Climatology Project

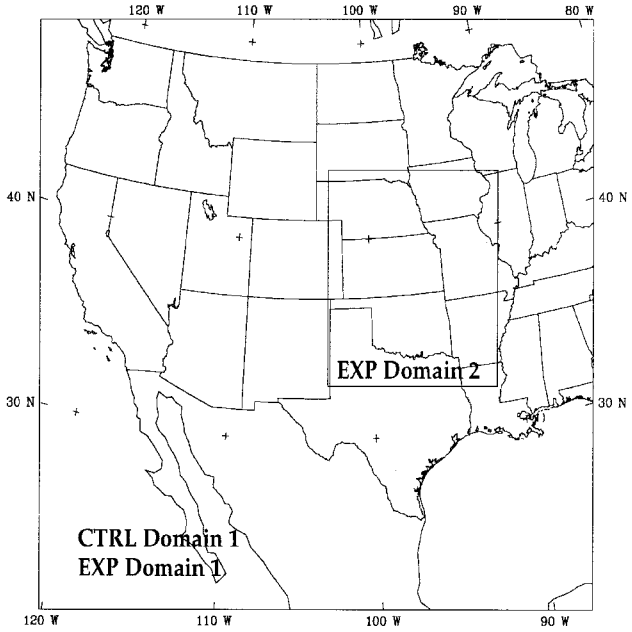

Figure 1. Domains used for simulation EXP. Simulation CTRL used only the outer domain. The coarse-grid domain is 91x99, with 36-km grid point separation; the fine grid domain is 100x91 and has 12-km grid spacing.

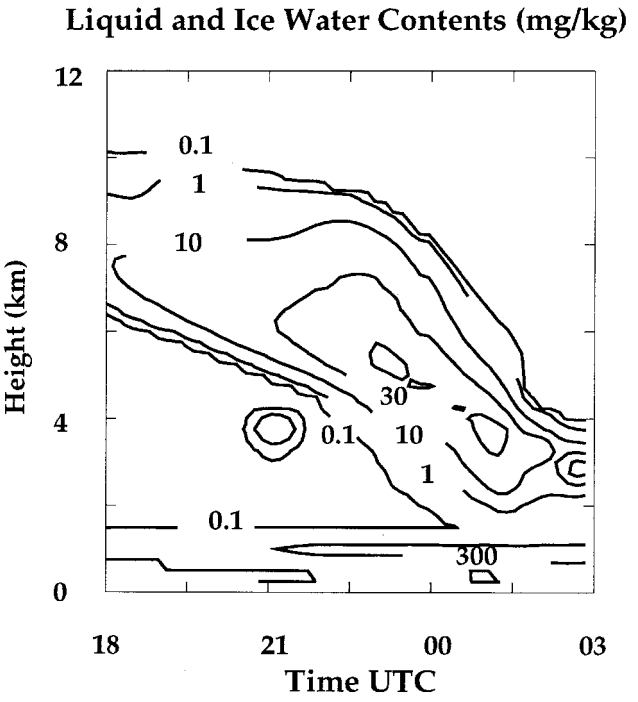

Figure 2. Model solutions of cloud water contents (CWC) every 10 min over Coffeyville, from EXP domain 2, 18 UTC to 00 UTC 27 November; for clarity, contour levels above 2 km are 0.1, 1, 10, 30, 60, and 300 mg kg^{-1}; below 2 km, contours are 0.1 and 300 mg kg^{-1}.

for the length of the Intensive Observation Period (IOP) of the FIRE-II experiment that ran from 12 UTC November 25 to 00 UTC 27 November 1991.

The coarse-grid domains of CTRL and EXP both simulate the main features of the case fairly well, although there is a lag of approximately 3 hr by the 00 UTC 27 November 1991 time. This lag is evident in the dynamical features, including the ridge-trough system and the jet streak, as well as the cloud field (not shown). Although both simulations over-forecast the cloud shield, the main features of interest resolvable by this domain are reproduced, including the general cloud shield structure, the clearing between the two cirrus systems, and the orientation of the main cloud band passing through Oklahoma. Both simulations generate gravity waves oriented NE-SW over the central U.S. (not shown). The fact that both simulations produce these gravity waves is an indication that these waves are not to be attributed to boundary effects from the second domain.

A time-height section of the second domain cloud and vertical velocity (Figure 2) over Coffeyville is provided for comparison with the PSU 94-FHZ radar returns from 18 UTC 26 November to 00 UTC 27 November (Mace et al. 1995). To correct for the lag, simulation EXP was integrated 3 hr past this time to determine if the model would capture the structure shown in the radar observations. With this additional information, the agreement between the structures of the observed and the model-simulated time-height sections is good, with some exceptions. The lower-tropospheric stratus deck appears too early (Figure 2) and is overforecasted compared with observations (not shown). The sudden drop in cloud base is found in the model solution, although the observed cloud top drops more precipitously than the model-resolved cloud. Thus, the main features are reproduced by the model, including the thickening and subsequent lowering of the cloud deck with time.

A time-height section through a point 240 km north of Coffeyville (not shown) reveals a much thicker cloud deck, with larger cloud water contents (CWC), throughout this period. This is consistent with observations and with the simulation by Westphal et al. (1996). This indicates that the model may be resolving cloud structures that agree with the reflectivities recorded by the radar, although it is displacing this cloud too far to the north.

Discussion of Simulated Gravity Waves

The gravity waves detected in the coarse domain are examined in greater detail using the 12-km resolution of Domain 2 simulation EXP. The simulated waves enter the domain by approximately 01 UTC 26 November and are characterized by a NE-SW orientation. The waves appear to propagate southeastward. Of the waves resolvable within this domain, two separate sets are long-lived and also show a significant impact on the development of the cloud structure. These waves, denoted A (Figure 3) and B (not shown) appear to propagate fully developed for several hours between 12 UTC 26 November and the end of the IOP at 00 UTC 27 November. The vertical extent of the upward motions of both waves spans several kilometers throughout the time of the waves' existence.

Calculation shows that both waves have ground relative phase speeds that have a westerly component, but their true phase speeds are oriented backwards against the mean flow. Periods of 2.6 hr for wave A and 2.0 hr for wave B are calculated. The waves are hydrostatic internal gravity waves, but could be considered inertia-gravity waves because their periods are close to the e-folding time of the Coriolis term (approximately 3 hr).

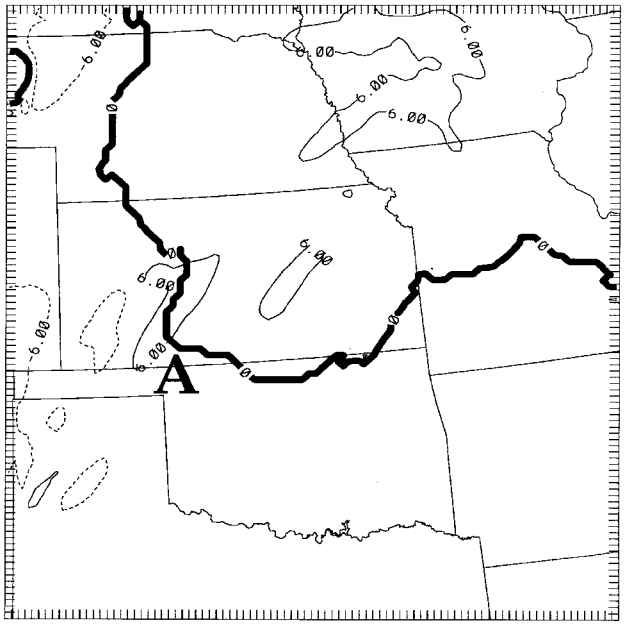

Figure 3. Areas of cloud at 500 mb, 18 UTC 26 November, in conjunction with vertical velocity. Contour for cloud is 0.1 mg kg^{-1}, and for vertical velocity 6 and -6 cm s^{-1}.

These wave properties are important in considering the development of the features of the cirrus system described by Mace et al. (1995). The satellite imagery of the 18 UTC cloud shows a NE-SW-oriented patch of cirrus over south central Kansas (not shown). By 21 UTC, according to their study, the cirrus had developed three wave-like bands.

The vertical velocity field for 18 UTC 500 mb reveals the presence of wave A within the cloud boundary (Figure 3). This wave corresponds to the main "bulge" resolved in the satellite photo at this time; the wave has apparently forced this spur since its inception at 12 UTC. The relative humidity with respect to liquid (not shown) is dryer behind the cloud system; this explains the cloud-free region despite strong upward motions in that vicinity. By 20 UTC, wave A has propagated southeastward relative to the ground. However, as the phase velocities indicate, this wave is traveling upstream relative to the mean flow; the cloud field is traveling with the mean flow, and thus the wave is effectively propagating away from the cloud. By 21 UTC, the wave is completely separated from the main cloud portion; the spur, however, remains. Animation of the imagery shows that this spur appears to advect with the mean flow, losing its NE-SW tilt, until approximately 00 UTC 27 November when it either dissipates or is advected into the main body of the cloud. It is also important to note that other waves, although less long-lived than wave A, are responsible for cloud bands throughout various segments of the simulation; their impact is much the same as that described for wave A. The results of this model simulation give evidence that the wave-like cloud bands described by Mace et al. (1995) are due to the upward motions of the NE-SW tilted gravity waves. These waves, with phase speeds oriented against the mean flow, then propagate behind the cloud into the dryer air. Thus, the cloud bands are left behind, and their southern tips can be advected faster by the jet streak than their northern portions as described in the Mace et al. study, explaining the entire progression of the cloud bands.

Uccellini and Koth (1987) related thirteen independent case studies of long-lived gravity wares, characterized by periods of 1-4 hr and horizon wavelengths of 50-500 km, to synoptic characteristics. This study quantified boundaries for an area of preferred excitation of gravity waves; a jet streak axis formed the west/northwest boundary, with a surface front to the southeast, a trough-ride inflection axis to the southwest, and a ridge axis to the northeast. These factors are all present for the time being simulated, although the placement of the various features is transposed (Figure 4). As the jet streak

propagates, so does the "box," and the gravity wave activity should shift eastward. This is noted in the simulation. The presence of these waves in areas predicted by the Uccellini and Koch study provides a basis for hypothesizing jet-streak-excited gravity waves. However, the specific source mechanism must be addressed. According to Uccellini and Koch, geostrophic adjustment occurring in the vicinity of the jet and vertical shear instability are the two likely mechanisms. Calculation of Rossby radii of deformation for a stratified atmosphere (Blumen 1972), as well as the wavelengths that could be expected from vertical shear instability, led them to postulate that the geostrophic adjustment mechanism was the source of the waves in their study.

Calculations of these quantities from model-simulated data of the IOP support this finding; the Rossby radii of deformation (on the order of 150 km) were equal to or slightly larger than the wavelengths found for waves A and B (on the order of 125 km). Also, expected wavelengths calculated within maximum wind shear regions of the jet exit region cluster around 25 km. This is much smaller than the simulated wavelengths, and thus, vertical shear instability is not a likely source. Therefore, geostrophic adjustment is more likely.

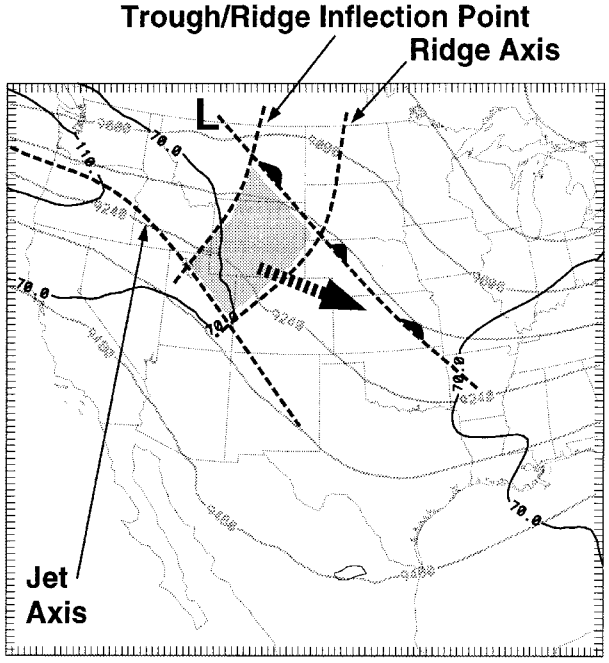

Figure 4. Preferred areas for gravity wave activity based on synoptic features at 00 UTC 26 November. Arrow denotes direction of propagation of the jet streak. After Uccellini and Koch (1987).

Conclusions

The generating source and mechanism of the gravity waves simulated in the model have been hypothesized. The calculation of the Rossby radii of deformation, comparison to wavelengths of shear-induced waves, and periods of the simulated waves lend credence to the postulation of the jet streak's geostrophic adjustment as the source. However, a definitive study of the waves' characteristics must be done in order to isolate this feature as the cause of these waves. Specifically, an analysis of the group velocity of these waves would provide more evidence that they are indeed jet streak related. The possibility of mountain wave influence in the generation of the gravity waves must also be addressed, as well as the longevity of the waves.

Wave A was shown to have a significant impact on the cloud structure. In-depth examination of gravity wave impacts on cirrus microphysical structure is necessary to assess the accuracy of the treatment of these clouds in parameterizations. More study needs to be done to determine if the treatment of cirrus clouds on the large scale is insufficient for resolving their actual impacts on the climate.

Acknowledgments

This work was supported under U.S. Department of Energy grant number DE-FG02-90ER-61071.

References

Blumen, W., 1972: Geostrophic adjustment. *Rev. Geophys. Space Phys*., **10**, 485-528.

Bougeault, P., 1983: A non-reflective boundary condition for limited-height hydrostatic models. *Mon. Wea. Rev*., **111**, 420-429.

Dudhia, J., 1993: A non-hydrostatic version of the Penn State-NCAR mesoscale model: Validation tests and simulations of an Atlantic cyclone and cold front. *Mon. Wea. Rev*., **121**, 1493-1513.

Grell, G., J. Dudhia, and D. Stauffer, 1994: *A Description of the Fifth-Generation Penn State/NCAR Mesoscale Model (MM5)*. NCAR Technical Note, **42**, National Center for Atmospheric Research, Boulder, Colorado.

Gultepe, I., and D. O. Starr, 1995: Dynamical structure and turbulence in cirrus clouds: Aircraft observations during FIRE. *J. Atmos. Sci*., **52**, 4159-4182.

Heymsfield, A., and L. Donner, 1990: A scheme for parameterizing ice-cloud water content in general circulation models. *J. Atmos. Sci*., **47**, 1865-1877.

Klemp, J., and D. Durran, 1983: An upper boundary condition permitting internal gravity wave radiation in numerical mesoscale models. *Mon. Wea. Rev*., **111**, 430-444.

Mace, G., D. O'C. Starr, T. Ackerman, and P. Minnis, 1995: Examination of coupling between an upper-tropospheric cloud system and synoptic-scale dynamics diagnosed from wind profiler and radiosonde data. *J. Atmos. Sci*., **52**, 4094-4127.

Meyers, M., P. Demott, and W. Cotton, 1992: New primary ice-nucleation parameterizations in an explicit cloud model. *J. Applied Meteorol*., **31**, 708-721.

Reisner, J., R. Rasmussen, and R. Bruintjes, 1996: Explicit forecasting of supercooled liquid water in winter storms using a mesoscale model. *J. Applied. Meteorol*., (submitted).

Sassen, K., D. O'C. Starr, and T. Uttal, 1989: Mesoscale and microscale structure of cirrus clouds: Three case studies. *J. Atmos. Sci*., **46**, 371-396.

Stauffer, D., and N. Seaman, 1990: Use of four-dimensional data assimilation in a limited-area mesoscale model. Part I: Experiments with synoptic-scale data. *Mon. Wea. Rev*., **118**, 1250-1277.

Uccellini, L., and S. Koch, 1987: The synoptic setting and possible energy sources for mesoscale wave disturbances. *Mon. Wea. Rev*., **115**, 721-729.

Uttal, T., E. Clothiaux, T. Ackerman, J. Intrieri, and W. Eberhard, 1995: Cloud boundary statistics during FIRE-II. *J. Atmos. Sci*. **52**, 4264-4275.

Westphal, D., S. Kinne, P. Pilewskie, J. Alvarez, S. G. Benjamin, W. L. Eberhard, A. J. Heymsfield, R. A. Kropfli, G. G. Mace, S. Y. Matrosov, S. H. Melfi, P. Minnus, J. B. Snider, B. J. Soden, D. O'C. Starr, T. A. Uttal, and D. F. Young, 1996: Initialization and Validation of a Simulation of Cirrus Using FIRE-II Data. *J. Atmos. Sci*., **53**, 3397-3429.